
A Space-Time Transformer for Precipitation Forecasting

Levi Harris
 UNC Chapel Hill
 levlevi@cs.unc.edu

Tianlong Chen
 UNC Chapel Hill
 tianlong@cs.unc.edu

Abstract

Meteorological agencies around the world rely on real-time flood guidance to issue live-saving advisories and warnings. For decades traditional numerical weather prediction (NWP) models have been state-of-the-art for precipitation forecasting. However, physically-parameterized models suffer from a few core limitations: first, solving PDEs to resolve atmospheric dynamics is computationally demanding, and second, these methods degrade in performance at nowcasting timescales (i.e., 0-4 hour lead-times). Motivated by these shortcomings, recent work proposes AI-weather prediction (AI-WP) alternatives that learn to emulate analysis data with neural networks. While these data-driven approaches have enjoyed enormous success across diverse spatial and temporal resolutions, applications of video-understanding architectures for weather forecasting remain underexplored. To address these gaps, we propose **Satformer**: a video transformer built on full space-time attention that skillfully forecasts extreme precipitation from satellite radiances. Along with our novel architecture, we introduce techniques to tame long-tailed precipitation datasets. Namely, we reformulate precipitation regression into a classification problem, and employ a class-weighted loss to address label imbalances. Our model scored **first place** on the NeurIPS Weather4Cast 2025 “Cumulative Rainfall” challenge. Code and model weights are available: github.com/leharris3/satformer

1 Introduction

Extreme precipitation poses outsized risks to life, property, and commerce. Recent studies predict that these events are likely to increase in frequency and severity during the coming decades, spurred on by a warming atmosphere [16, 22]. Timely and accurate public advisories save lives and allow interested parties to make appropriate preparations for future weather events. However, traditional sources of operational forecast guidance are plagued by key limitations. First, numerical weather prediction (NWP) models like the operational ECMWF incur enormous computational costs. And second, these models are often only available at hourly time-scales, and are therefore inappropriate sources of real-time guidance.

Recent data-driven, so-called AI-weather prediction (AI-WP) approaches offer a compute-efficient alternative to NWP models by learning to emulate forecast analysis data. Breakthrough works from Google [19, 26], NVIDIA [24], Huawei [5], and others replace core components of the weather-prediction pipeline with neural networks. These learning-based methods have manifold advantages. Namely, AI-WP pipelines can practically run at sub-hourly intervals and in large ensembles; researchers are therefore optimistic that operational meteorologists can one day leverage these models as a source of real-time guidance and robust uncertainty estimation. However, previous studies primarily explore AI-WP for medium-range forecasting on a global scale. This is a natural choice given the surplus of historical data available at these resolutions. By contrast, forecasting extreme precipitation at nowcasting timescales is a nascent area of research.

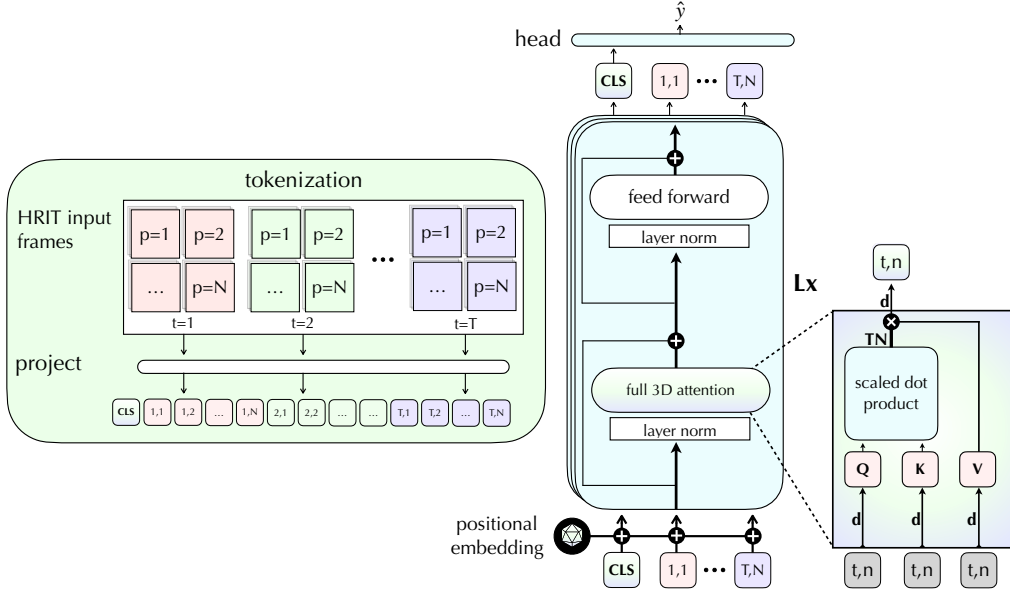


Figure 1: The SaTformer architecture. (Left) We partition each frame $t \in (1, \dots, T)$ in a sequence of satellite radiances into N non-overlapping patches. Each patch is projected into a token representation, and a class token (CLS) is prepended to the token sequence. (Center) Model encoder design. Token sequences pass through (L) transformer layers. The class token is spliced from the output of the final transformer layer and passed to a single-layer prediction head. (Right) Full 3D attention; all tokens attend to all tokens over time and space.

This work aims to develop a solution to the NeurIPS Weather4Cast 2025 “Cumulative Rainfall” challenge. Here, we predict future rainfall quantities from HRIT satellite radiance inputs. In practice, this task is formulated as a video to scalar regression problem. An added set of obstacles therefore exists to apply methods from video understanding literature (which offers a wealth of methods for classification, but not single-value regression-problems) to this unique task. Motivated by these challenges, we seek answers to the following research questions:

1. What modifications are required to adapt video understanding architectures for cumulative precipitation estimation?
2. What techniques support model skillfulness (e.g., calibration, performance on extremes, etc) when training on long-tailed precipitation datasets?

To investigate the points above, we propose **SaTformer**: a full attention video transformer for extreme precipitation forecasting using low-resolution satellite imagery as input. Unlike prior deep learning solutions for precipitation regression, our approach is entirely end-to-end and eschews bespoke architecture choices that are unlikely to generalize to new domains. Moreover, we evaluate various strategies (including task-reformulations and a class-balanced loss function) designed to tame imbalanced datasets and encourage skill parity for forecasting common and extreme precipitation events.

2 Background

2.1 Weather4Cast competition

Beginning in 2021, the annual Weather4Cast competition (W4CC) evaluates machine learning (ML) techniques for weather forecasting within spatial and temporal transfer learning regimes [11, 12]. Each year, participants are tasked with developing approaches to predict unseen (OPERA) high-resolution radar precipitation fields (or targets derived from these data) using 11-band HRIT geostationary satellite data and static topographic maps as context. Competition data cover 10,

non-overlapping regions (spatial areas of 1512×1512 km) across Europe, northern Africa, and the middle-east for which HRIT data are completely available, while OPERA data are sparse.

3 Related work

Motivated by strong overlaps between subsequent task variations, we review works from all preceding years of the W4CC.

3.1 W4CC 2021

In its inaugural year organizers proposed a multivariate weather forecasting challenge: participants predicted future atmospheric states (represented by four variables) for eight hours of lead-time using the same features and topographic information as model inputs [18]. The authors of [18] proposed to solve this task by training a U-Net VAE with a combination of deterministic and probabilistic losses. In this work it is argued that these design choices are crucial for modeling the fundamental uncertainty (i.e., aleatoric and epistemic) present in weather forecasting and that they therefore aid model performance. However, this complex, multi-loss setup may prove difficult to extend to new tasks in practice.

3.2 W4CC 2022

In 2022 the multi-variate challenge from 2021 was replaced by a uni-variate, binary precipitation forecasting task defined for 64×64 km OPERA radar-regions and 8 hours of lead-time.

In [3] an ensemble of video classification models (e.g., Swin UNETR, ViViT) is presented [1, 15]). An obvious drawback is that this approach requires training three different models from scratch for a single task and incurs further computational costs by bootstrapping predictions at inference-time. Additionally, modifications made by the authors to adopt video classification models to a video generation task (e.g., appending a single convolutional layer to ViViT to predict the output temporal dimension) are likely brittle design choices. In [21], the authors apply a 3D U-Net and an Earthformer [6, 9] to solve this year’s stage 1 and stage 2 challenges, respectively. In the second challenge, an Earthformer is employed to efficiently decompose a video-sequence into cuboids (as opposed to frame-wise patches as proposed in ViT); self-attention is performed between cuboids and a collection of global context tokens \mathcal{G} . However, inter-cuboid attention is axial, and therefore, cuboids only learn spatial dependencies from a set of coarse global context vectors.

Beginning with a standard 3D U-Net, the authors of [23] introduce a time-space (TS) convolutional block in which a spatial convolution, followed by a “temporal-wise dilated convolution” (TSDConv), and finally a temporal convolution are applied to the input feature maps. The authors note that their proposed TSDConv is simply an extension of the large kernel convolution operation into three dimensions. Additionally, WeatherFusionNet [25] propose a physically informed U-Net-based architecture. Their model as inputs uses HRIT satellite radiances, a PDE-constrained video prediction via PhyDNet [13], and the outputs of a proposed Sat2Rad module to forecast binary rain masks. While the methods above achieve strong performance on W4CC tasks, most are fundamentally reliant on CNN model designs, and likely suffer from the inductive biases and poor scaling these architectures exhibit in other domains.

3.3 W4CC 2023

Tasks did not change between 2022 and 2023.

This year, researchers at Alibaba Cloud proposed a mixture-of-experts-inspired-solution to both the “core” and “transfer learning” competition tracks [20]. The authors design a “predictor”, which samples multiple times from a WeatherFusionNet backbone, and a “controller”; the latter module produces a final output as a weighted combination of the expert predictions. In addition to being a minor extension of prior works, the proposed model employs an arduous three-stage training scheme. The aforementioned work is still preferable to [17], who simply finetune a NowcastNet [28] on the challenge dataset. In [14] an augmentation technique is proposed to sample linear interpolations of the original training samples. By formulating precipitation forecasting as a multi-class, video classification task (where each per-pixel class represents a discrete interval of precipitation, the

authors may employ a modified dice-loss with an added ordinal prior (i.e., under-predictions are punished more heavily than over-predictions). While certainly performant, this approach is heavily engineered and therefore may generalize poorly to new tasks and datasets

3.4 W4CC 2024

In 2024, the W4CC organizers shortened the duration of target OPERA sequences from 8 hours to 4 hours.

[7] develop a conditional GAN network trained on a sparsely-sampled subset of the original HRIT channels. Here, the authors completely discard near-infrared, water vapor, and visible satellite data, and average the remaining 4 channels; after data preprocessing their model is trained on only single-channel inputs. Further preprocessing techniques are employed to improve model performance: including thresholding out non-cloudy regions and extracting optical flow scores from the input sequence. Similar to [14], this work proposes a bespoke, highly-engineered pipeline that is unlikely to extend gracefully to future work.

4 Method

4.1 SaTformer model

Taking inspiration from video understanding literature, we introduce a transformer-based architecture for precipitation estimation (Fig. 1). Given one hour of low-resolution HRIT satellite data $\mathbf{x} \in \mathbb{R}^{T \times C \times H \times W}$, our model learns a mapping to cumulative rainfall targets $f_\theta(\cdot) \mapsto y$ where $y = \{0, 1\}^n$ is a categorical approximation using n bins of y_{reg} : the target label provided by the organizers (Eq. 9).

Following prior work [4, 8], we partition each frame in the input sequence into $N = HW/P^2$ non-overlapping patches with side-length P indexed at timestep $t \in 1, \dots, T$ and spatial index $p \in 1, \dots, N$: $\mathbf{x}_{(t,p)}^{(0)} \in \mathbb{R}^{P \times P \times C}$; patches completely cover the spatial dimensions of the original frame. We flatten each patch, then project the resulting vectors into tokens: $\mathbf{z}'_{(t,p)}^{(0)} \in \mathbb{R}^d$. We prepend a randomly initialized “class token” $\mathbf{z}'_{(0,0)}^{(0)}$ to the token sequence intended to aggregate relevant information for prediction of the target label:

$$[\mathbf{z}'_{(0,0)}^{(0)}, \mathbf{z}'_{(1,1)}^{(0)}, \dots, \mathbf{z}'_{(T,N)}^{(0)}] \quad (1)$$

We add learnable positional embeddings $\mathbf{e}_{(t,p)} \in \mathbb{R}^d$ to all $NT + 1$ tokens in the input sequence:

$$\mathbf{z}_{(0,0)}^{(0)} = \mathbf{z}'_{(0,0)}^{(0)} + \mathbf{e}_{(0,0)} \quad \mathbf{z}_{(t,p)}^{(0)} = \mathbf{z}'_{(t,p)}^{(0)} + \mathbf{e}_{(t,p)} \quad (2)$$

4.1.1 Full space-time self-attention

Our model is composed of L transformer encoder blocks $l \in 1, \dots, L$ that sequentially operate on the input token sequence. To quickly capture rich, long-distance dependencies over time and space, we implement full space-time self-attention. Here, each token in the input sequence is mapped to a query, key, and value vector using respective weight matrices $W \in \mathbb{R}^{d \times d}$:

$$\mathbf{q}_{(t,p)}^{(l)} = \text{LN}(\mathbf{z}_{(t,p)}^{(l-1)})W_q \quad \mathbf{k}_{(t,p)}^{(l)} = \text{LN}(\mathbf{z}_{(t,p)}^{(l-1)})W_k \quad \mathbf{v}_{(t,p)}^{(l)} = \text{LN}(\mathbf{z}_{(t,p)}^{(l-1)})W_v \quad (3)$$

Where $\mathbf{q}_{(t,p)}^{(l)} \in \mathbb{R}^d$, $\mathbf{k}_{(t,p)}^{(l)} \in \mathbb{R}^d$, $\mathbf{v}_{(t,p)}^{(l)} \in \mathbb{R}^d$ and $\text{LN}(\cdot)$ denotes the LayerNorm operation [2]. Next we compute importance weights $\mathbf{a}_{(t,p)}^{(l)}$ between all pairs of tokens across time and space:

$$\mathbf{a}_{(t,p)}^{(l)} = \text{softmax}\left(\frac{(\mathbf{q}_{(t,p)}^{(l)})^\top}{\sqrt{d}} \cdot [\mathbf{k}_{(0,0)}^{(l)}, \mathbf{k}_{(1,1)}^{(l)}, \dots, \mathbf{k}_{(T,N)}^{(l)}]\right) \quad (4)$$

where $\mathbf{a}_{(t,p)}^{(l)} \in \mathbb{R}^{TN+1}$. The output of the self-attention layer is a weighted sum calculated between all value vectors and importance weights for each token:

$$\mathbf{s}_{(t,p)}^{(l)} = \mathbf{a}_{(t,p)(0,0)}^{(l)} \mathbf{v}_{(0,0)}^{(l)} + \sum_{t'=1}^T \sum_{p'=1}^N \underbrace{\mathbf{a}_{(t,p)(t',p')}^{(l)}}_{\text{scaler}} \mathbf{v}_{(t',p')}^{(l)} \quad (5)$$

where $\mathbf{s}_{(t,p)}^{(l)} \in \mathbb{R}^d$. The resulting attention scores are projected and summed with a residual connection from the previous encoder block; these resulting vectors are passed through the remainder of the transformer layer:

$$\mathbf{z}'_{(t,p)}^{(l)} = s_{(t,p)}^{(l)} W_{\text{out}} + \mathbf{z}_{(t,p)}^{(l-1)} \quad \mathbf{z}_{(t,p)}^{(l)} = \text{MLP}(\text{LN}(\mathbf{z}'_{(t,p)}^{(l)})) + \mathbf{z}'_{(t,p)}^{(l)} \quad (6)$$

Note that in practice we employ a standard transformer encoder-design implemented with multi-headed attention; notation for multi-headed attention is omitted for brevity.

4.1.2 Categorical task formulation

Deep neural networks often struggle to match the performance of ML baselines on regression tasks, particularly within imbalanced data regimes [10, 27]. To address these challenges and to exploit proven model designs for classification tasks, we reformulate precipitation regression as a classification problem. Given a target regression label $y_{\text{reg}} \in \mathbb{R}$ and a training dataset \mathcal{D} , we approximate categorical equivalent labels by partitioning the target space into n , non-overlapping sub-intervals with step size δ :

$$(\mathcal{D}_{y_{\text{min}}}, \mathcal{D}_{y_{\text{min}} + \delta}, \dots, \mathcal{D}_{y_{\text{min}} + i\delta}, \dots, \mathcal{D}_{y_{\text{max}}})_{i=0 \dots n-1}$$

We then generate one-hot categorical labels $y \in \{0, 1\}^n$, representing a bin centered at $\mathcal{D}_{y_{\text{min}} + i\delta}$, by calculating the nearest label-bin to a target: $i = \text{round}(\frac{y_{\text{reg}} - \mathcal{D}_{y_{\text{min}}}}{\delta})$. Our model learns to predict categorical labels derived above. Taking the output of the last transformer encoder block, we splice out the ultimate class token $\mathbf{z}_{(cls)}^{(L)}$; a one-layer MLP prediction head generates class-probabilities using this token as input.

$$\hat{y} = \text{softmax}(\text{MLP}(\mathbf{z}_{(cls)}^{(L)})) \quad (7)$$

4.1.3 Class-weighted cross-entropy loss

Extreme precipitation events are rare events, naturally. Standard classification loss functions (e.g., cross-entropy) bias models in favor of majority classes, degrading performance on long-tailed datasets like ours (Fig. 2). We employ a reweighted categorical cross entropy loss to offset class imbalances and promote model skill when forecasting outlier events:

$$\mathcal{L}(y, \hat{y}) = - \sum_{i=1}^n w_i \log(\hat{y}_i) y_i \quad (8)$$

Here \hat{y} is our model’s predicted probability distribution over the target classes and $w_i = -\log(\frac{||\mathcal{D}_i||}{||\mathcal{D}_{\text{total}}||})$ is the log-scaled relative frequency of a class in the training set.

5 Experiments

5.1 W4CC 2025: cumulative rainfall estimation

Our work solves the “Cumulative Rainfall” task from W4CC 2025. This year’s task involved prediction of cumulative precipitation targets from 11-band satellite imagery spanning visible, infrared,

and water vapor channels. Given 1 hour of HRIT satellite imagery, $\mathbf{x} \in \mathbb{R}^{T \times C \times H \times W}$, where T , C , H , and W represent the temporal, channel, height, and width dimensions of the input tensor, respectively, target labels y_{reg} are derived from a 4 hour sequence of OPERA high-resolution rain rate fields $\mathbf{r} \in \mathbb{R}^{T' \times H' \times W'}$ proceeding the input, and sharing the same spatial center point. The organizers state this target can be derived by: “[averaging] over a 32×32 pixel area...averaging the 16 slots and multiplying by 4 (or summing the 16 slots and diving [sic] by 4)”:

$$y_{\text{reg}} = \frac{4}{T'W'H'} \sum_{t=1}^{T'} \sum_{i=1}^{H'} \sum_{j=1}^{W'} \mathbf{r}_{(t,i,j)} \quad (9)$$

5.2 Dataset

We train our model using 7, region-specific datasets provided by the W4CC organizers containing pairs of HRIT satellite radiances and OPERA precipitation fields. At each step in our training process, we select a random region r from our dataset. Within this region, we randomly sample a 32×32 pixel (512×512 km) spatial crop HRIT sample for a random, four-consecutive frame (1 hour) temporal window. This subsample comprises our model input tensor \mathbf{x}_{raw} . We then select a 32×32 pixel (64×64 km) OPERA sample centered at the geographic point as \mathbf{x}_{raw} and spanning the 16 frames (4 hours) proceeding the model input data. As previously denoted, we refer to this subsample as \mathbf{r} . We can then derive model targets y_{reg} using the formulation in equation (9). Next, we normalize all input features roughly between $[0, 1]$ using statistics calculated over our training set.

$$\mathbf{x} = \frac{\mathbf{x}_{\text{raw}} - \mathcal{D}_{\text{xmin}}}{\mathcal{D}_{\text{xmax}} - \mathcal{D}_{\text{xmin}}}$$

5.3 Training details

We configure our SaTformer with input height and width 32, channel dimension 11, number of classes 64, patch size 4, hidden dimension 512, head dimension (for multi-headed attention) 64 using 8 heads, total transformer encoder blocks ($L=12$), initialized with learnable positional embeddings. We train our model for 200 epochs and a total of 25,000 steps using the Adam optimizer configured with a learning rate 1e-5, and an effective batch size 128 on $4 \times \text{A6000}$ GPUs. We evaluate model checkpoints that score the lowest average validation loss during a training run.

5.4 Results

All models entered in W4CC 2025 are evaluated using cumulative ranked probability score (CRPS). For each input sequence in the test set, model-predicted cumulative mass functions $F_{\theta}(\hat{y})$ are compared against a degenerate, ground-truth distribution over n bins:

$$CPRS(F_{\theta}, y) = \sum_{i=1}^n \left(F_{\theta}(\text{bin}_i) - \mathbb{1}(y \leq \text{bin}_i) \right)^2$$

where bin_i denotes the quantity for the i -th precipitation bucket. Our best performing model achieves a CRPS score of 3.135 on the challenge set, ranking in **first place** in the W4CC 2025 “Cumulative Rainfall” challenge.

5.5 Ablation study

We conduct ablations for several design choices made throughout this paper. Concretely, our SaTformer can be derived step-by-step from a TimeSformer baseline [4] implemented with interleaved space-time attention modules and trained via standard CCE loss. As previously mentioned, datasets for extreme weather forecasting commonly suffer from large class imbalances. As shown in Figure 2 our target distribution is heavily skewed towards low/no rain events and contains large gaps in sample coverage at the extremes. To encourage balanced performance across classes we implement the weighted CCE loss proposed in equation (8); ablations performed using bin-averaged metrics

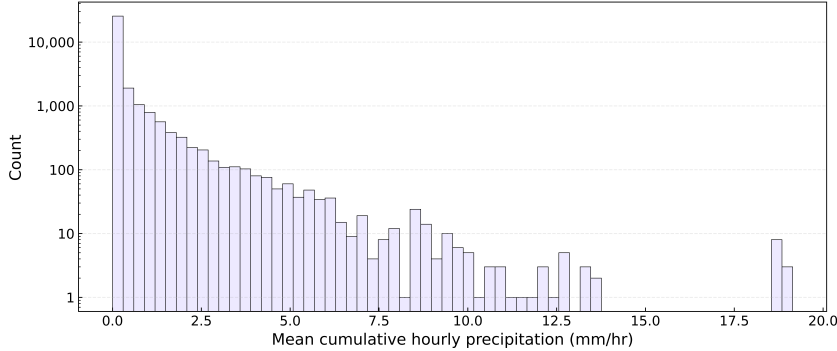


Figure 2: Empirical distribution of target labels within our training set. Note the log scale on the y-axis; targets for our task are skewed heavily towards low/no rain events.

Table 1: Ablations conducted on the W4CC validation set. To assess model skill on poorly represented classes (i.e., extreme precipitation events) we develop bin-weighted (BW) variants of standard regression and classification metrics. Here, we report class averaged model accuracy (BW-Top-3) and CRPS scores. (Top) We compare model performance with and without class-frequency re-weighting. When using a standard CCE loss our model quickly overfits to low/no-rainfall events. (Bottom) Comparison of three attention variants: space followed by time ($S \rightarrow T$), time then space ($T \rightarrow S$), and full space-time self-attention ($S + T$).

Loss weighting?	BW-Top-3 \uparrow	BW-CRPS \downarrow
-	0.076	6.91
✓	0.272	2.64
Attention		
$S \rightarrow T$	0.250	4.39
$T \rightarrow S$	0.214	3.39
$S + T$	0.272	2.64

confirm that including a class-frequency prior from the training distribution greatly aids model skill (Table 1).

A large departure we make from prior video understanding works is to implement full 3D attention in our transformer encoder layers. Complex video reasoning tasks (e.g., action recognition) typically require high-temporal and spatial resolution inputs. However, the input satellite radiances provided to us by the organizers span just 4 frames, and require attention over a much smaller pixel-area than is common for natural videos. Full space-time attention allows our model to quickly capture rich, long-distance dependencies over space and time. Ablations comparing various attention implementations confirm that full space and time attention yields superior model performance (Table 1) on our cumulative precipitation estimation task.

Satisfied with our choice of loss function and encoder design, we conclude evaluations to determine optimal bin-size using the W4CC challenge set. We note that while choosing to predict more output classes (i.e., using smaller values of δ) generally yields better CRPS scores in theory, in practice models tend to produce degenerate solutions as class representation becomes increasingly sparse. A reasonable middle ground of 64 classes achieves the best empirical results (Table 2).

6 Discussion

6.1 RQs

We briefly return to the research questions posed at the beginning of this paper.

Table 2: W4CC challenge set scores for increasingly fine-grained precipitation buckets.

# Bins	CRPS ↓
4	14.181
8	5.987
16	4.293
32	3.898
64	3.135
128	3.610
256	5.312
512	4.783

“What modifications are required to adapt video understanding architectures for cumulative precipitation estimation?”

We find that video classification models perform remarkable well on cumulative rainfall prediction tasks with minimal modification. Empirically, we find that we can improve upon model baselines by ablating the number of output classes (Table 1). Another task-specific modification we make is to implement full self-attention over space and time. This traditionally computationally expensive design-choice is made possible due to the small spatial dimensions of our input sequences. Researchers hoping to apply transformers to higher dimensional weather data may require alternative methods that scale linearly or sub-linearly with respect to the size of the input sequence.

“What techniques support model skillfulness (e.g., calibration, performance on extremes, etc when training on long-tailed precipitation datasets?”

As shown in Table 1, partitioning the target space into discrete bins allows us to achieve optimal performance when applying video classification models to precipitation regression. Moreover, without additional calibration or class-regularization techniques, model performance can degrade towards degenerate solutions (i.e., always predict ‘no rain’) in imbalanced learning regimes. Our experiments show that a simple class-weighted cross entropy loss achieves meaningful gains compared to standard loss formulations. Taming long-tailed datasets like those explored in this paper remains a critical challenge in AI-WP. Future work may improve upon the results presented here by employing data augmentation techniques or by utilizing other task formulations that are robust to skewed datasets.

6.2 Limitations

Our proposed SaTformer achieves strong performance on a precipitation estimation task. However, significant modifications to our method may be required to produce complete forecasts (i.e., video-like outputs) over space and time. Researchers may consider using graph networks or diffusion-based approaches for auto-regressive prediction tasks instead. Additionally, full 3D attention (while a powerful mechanism for capturing space-time dependencies) incurs quadratic costs with respect to the length of the input sequence. Those interested in adopting our method to longer satellite videos may consider other efficient self-attention approaches (e.g., decoupled space-time attention, sparse self-attention, etc). Future work may also benefit by employing a self-supervised encoder to compress video inputs prior to the tokenization stage.

7 Conclusion

In this paper, we proposed SaTformer: a video transformer that can skillfully predict precipitation targets over fine space-time resolutions using low-resolution satellite imagery as input. We demonstrate that by combining a categorical task formulation and a class-weighted loss function, our model gains robust performance across high and low-frequency classes in an imbalanced learning paradigm. Moreover, we provide evidence that full space-time attention improves model performance in our domain, and thus may be a viable option in other low-token regimes. Our method demonstrates strong performance in empirical experiments and ranked first at the NeurIPS 2025 Weather4Cast “Cumulative Rainfall” challenge.

References

- [1] Anurag Arnab et al. *ViViT: A Video Vision Transformer*. 2021. arXiv: [2103.15691 \[cs.CV\]](https://arxiv.org/abs/2103.15691). URL: <https://arxiv.org/abs/2103.15691>.
- [2] Jimmy Lei Ba, Jamie Ryan Kiros, and Geoffrey E. Hinton. *Layer Normalization*. 2016. arXiv: [1607.06450 \[stat.ML\]](https://arxiv.org/abs/1607.06450). URL: <https://arxiv.org/abs/1607.06450>.
- [3] Yury Belousov, Sergey Polezhaev, and Brian Pulfer. *Solving the Weather4cast Challenge via Visual Transformers for 3D Images*. 2022. arXiv: [2212.02456 \[cs.CV\]](https://arxiv.org/abs/2212.02456). URL: <https://arxiv.org/abs/2212.02456>.
- [4] Gedas Bertasius, Heng Wang, and Lorenzo Torresani. *Is Space-Time Attention All You Need for Video Understanding?* 2021. arXiv: [2102.05095 \[cs.CV\]](https://arxiv.org/abs/2102.05095). URL: <https://arxiv.org/abs/2102.05095>.
- [5] Kaifeng Bi et al. “Accurate medium-range global weather forecasting with 3D neural networks”. In: *Nature* 619.7970 (July 2023), pp. 533–538. ISSN: 1476-4687. DOI: [10.1038/s41586-023-06185-3](https://doi.org/10.1038/s41586-023-06185-3). URL: [http://dx.doi.org/10.1038/s41586-023-06185-3](https://doi.org/10.1038/s41586-023-06185-3).
- [6] Özgün Çiçek et al. *3D U-Net: Learning Dense Volumetric Segmentation from Sparse Annotation*. 2016. arXiv: [1606.06650 \[cs.CV\]](https://arxiv.org/abs/1606.06650). URL: <https://arxiv.org/abs/1606.06650>.
- [7] Atharva Deshpande et al. *A conditional Generative Adversarial network model for the Weather4Cast 2024 Challenge*. 2024. arXiv: [2412.00451 \[cs.CV\]](https://arxiv.org/abs/2412.00451). URL: <https://arxiv.org/abs/2412.00451>.
- [8] Alexey Dosovitskiy et al. *An Image is Worth 16x16 Words: Transformers for Image Recognition at Scale*. 2021. arXiv: [2010.11929 \[cs.CV\]](https://arxiv.org/abs/2010.11929). URL: <https://arxiv.org/abs/2010.11929>.
- [9] Zhihan Gao et al. *Earthformer: Exploring Space-Time Transformers for Earth System Forecasting*. 2023. arXiv: [2207.05833 \[cs.LG\]](https://arxiv.org/abs/2207.05833). URL: <https://arxiv.org/abs/2207.05833>.
- [10] Léo Grinsztajn, Edouard Oyallon, and Gaël Varoquaux. *Why do tree-based models still outperform deep learning on tabular data?* 2022. arXiv: [2207.08815 \[cs.LG\]](https://arxiv.org/abs/2207.08815). URL: <https://arxiv.org/abs/2207.08815>.
- [11] Aleksandra Gruca et al. “Multi-task Challenges for Rain Movie Prediction on the Road to Hi-Res Foundation Models”. In: *OpenReview* (2024). NeurIPS 2024 Competition Track. URL: <https://openreview.net/forum?id=AZ9WzDxoTf>.
- [12] Aleksandra Gruca et al. “Weather4cast at NeurIPS 2022: Super-Resolution Rain Movie Prediction under Spatio-temporal Shifts”. In: *Proceedings of the NeurIPS 2022 Competitions Track*. Ed. by Marco Ciccone, Gustavo Stolovitzky, and Jacob Albrecht. Vol. 220. Proceedings of Machine Learning Research. PMLR, 28 Nov–09 Dec 2022, pp. 292–313. URL: <https://proceedings.mlr.press/v220/gruca23a.html>.
- [13] Vincent Le Guen and Nicolas Thome. *Disentangling Physical Dynamics from Unknown Factors for Unsupervised Video Prediction*. 2020. arXiv: [2003.01460 \[cs.CV\]](https://arxiv.org/abs/2003.01460). URL: <https://arxiv.org/abs/2003.01460>.
- [14] Lu Han et al. *Learning Robust Precipitation Forecaster by Temporal Frame Interpolation*. 2023. arXiv: [2311.18341 \[cs.LG\]](https://arxiv.org/abs/2311.18341). URL: <https://arxiv.org/abs/2311.18341>.
- [15] Ali Hatamizadeh et al. *Swin UNETR: Swin Transformers for Semantic Segmentation of Brain Tumors in MRI Images*. 2022. arXiv: [2201.01266 \[eess.IV\]](https://arxiv.org/abs/2201.01266). URL: <https://arxiv.org/abs/2201.01266>.
- [16] Maximilian Kotz, Anders Levermann, and Leonie Wenz. “The effect of rainfall changes on economic production”. In: *Nature* 601.7892 (Jan. 2022), pp. 223–227. ISSN: 1476-4687. DOI: [10.1038/s41586-021-04283-8](https://doi.org/10.1038/s41586-021-04283-8). URL: [http://dx.doi.org/10.1038/s41586-021-04283-8](https://doi.org/10.1038/s41586-021-04283-8).
- [17] Ajitabh Kumar. *Skilful Precipitation Nowcasting Using NowcastNet*. 2023. arXiv: [2311.17961 \[physics.ao-ph\]](https://arxiv.org/abs/2311.17961). URL: <https://arxiv.org/abs/2311.17961>.
- [18] Pak Hay Kwok and Qi Qi. *A Variational U-Net for Weather Forecasting*. 2021. arXiv: [2111.03476 \[cs.LG\]](https://arxiv.org/abs/2111.03476). URL: <https://arxiv.org/abs/2111.03476>.
- [19] Remi Lam et al. “Learning skillful medium-range global weather forecasting”. In: *Science* 382.6677 (Dec. 2023), pp. 1416–1421. ISSN: 1095-9203. DOI: [10.1126/science.adi2336](https://doi.org/10.1126/science.adi2336). URL: [http://dx.doi.org/10.1126/science.adi2336](https://doi.org/10.1126/science.adi2336).
- [20] Xinzhe Li et al. *Precipitation Prediction Using an Ensemble of Lightweight Learners*. 2023. arXiv: [2401.09424 \[physics.ao-ph\]](https://arxiv.org/abs/2401.09424). URL: <https://arxiv.org/abs/2401.09424>.

- [21] Yang Li et al. *Super-resolution Probabilistic Rain Prediction from Satellite Data Using 3D U-Nets and EarthFormers*. 2022. arXiv: [2212.02998 \[cs.CV\]](https://arxiv.org/abs/2212.02998). URL: <https://arxiv.org/abs/2212.02998>.
- [22] Gavin D. Madakumbura et al. “Anthropogenic influence on extreme precipitation over global land areas seen in multiple observational datasets”. In: *Nature Communications* 12.1 (July 2021). ISSN: 2041-1723. DOI: [10.1038/s41467-021-24262-x](https://doi.org/10.1038/s41467-021-24262-x). URL: [http://dx.doi.org/10.1038/s41467-021-24262-x](https://doi.org/10.1038/s41467-021-24262-x).
- [23] Jinyoung Park et al. *RainUNet for Super-Resolution Rain Movie Prediction under Spatio-temporal Shifts*. 2022. arXiv: [2212.04005 \[cs.CV\]](https://arxiv.org/abs/2212.04005). URL: <https://arxiv.org/abs/2212.04005>.
- [24] Jaideep Pathak et al. *FourCastNet: A Global Data-driven High-resolution Weather Model using Adaptive Fourier Neural Operators*. 2022. arXiv: [2202.11214 \[physics.ao-ph\]](https://arxiv.org/abs/2202.11214). URL: <https://arxiv.org/abs/2202.11214>.
- [25] Jiří Pihrt et al. *WeatherFusionNet: Predicting Precipitation from Satellite Data*. 2022. arXiv: [2211.16824 \[cs.CV\]](https://arxiv.org/abs/2211.16824). URL: <https://arxiv.org/abs/2211.16824>.
- [26] Ilan Price et al. “Probabilistic weather forecasting with machine learning”. In: *Nature* 637.8044 (Dec. 2024), pp. 84–90. ISSN: 1476-4687. DOI: [10.1038/s41586-024-08252-9](https://doi.org/10.1038/s41586-024-08252-9). URL: [http://dx.doi.org/10.1038/s41586-024-08252-9](https://doi.org/10.1038/s41586-024-08252-9).
- [27] Yuzhe Yang et al. *Delving into Deep Imbalanced Regression*. 2021. arXiv: [2102.09554 \[cs.LG\]](https://arxiv.org/abs/2102.09554). URL: <https://arxiv.org/abs/2102.09554>.
- [28] Yuchen Zhang et al. “Skilful nowcasting of extreme precipitation with NowcastNet”. In: *Nature* 619.7970 (July 2023), pp. 526–532. ISSN: 1476-4687. DOI: [10.1038/s41586-023-06184-4](https://doi.org/10.1038/s41586-023-06184-4). URL: [http://dx.doi.org/10.1038/s41586-023-06184-4](https://doi.org/10.1038/s41586-023-06184-4).